JGR Oceans

RESEARCH ARTICLE
10.1029/2020JC016757

The Role of Wind Stress in Driving the Along-Shelf Flow in the Northwest Atlantic Ocean

Jiayan Yang[1] and **Ke Chen**[1]

[1]Department. of Physical Oceanography, Woods Hole Oceanographic Institution, Woods Hole, MA, USA

Key Points:

- Wind stress forcing is important for the mean shelf circulation in the northwestern Atlantic Ocean and its seasonal variability
- This finding contrasts to the prevailing view that NWA along-shelf flow is mainly forced by the freshwater discharges from rivers/glaciers
- It aims to motivate further studies using OGCMs with both wind stress and freshwater forcings

Correspondence to:
J. Yang,
jyang@whoi.edu

Citation:
Yang, J., & Chen, K. (2021). The role of wind stress in driving the along-shelf flow in the northwest Atlantic Ocean. *Journal of Geophysical Research: Oceans*, *126*, e2020JC016757. https://doi.org/10.1029/2020JC016757

Received 11 SEP 2020
Accepted 26 MAR 2021

Abstract The along-shelf circulation in the Northwest Atlantic (NWA) Ocean is characterized by an equatorward flow from Greenland's south coast to Cape Hatters. The mean flow is considered to be primarily forced by freshwater discharges from rivers and glaciers while its variability is driven by both freshwater fluxes and wind stress. In this study, we hypothesize and test that the wind stress is important for the mean along-shelf flow. A two-layer model with realistic topography when forced by wind stress alone simulates a circulation system on the NWA shelves that is broadly consistent with that derived from observations, including an equatorward flow from Greenland coast to the Mid-Atlantic Bight (MAB). The along-shelf sea-level gradient is close to a previous estimate based on observations. The along-shelf flows exhibit strong seasonal variations with along-shelf transports being strong in fall/winter and weak in spring/summer, consistent with available observations. It is found that the NWA shelf circulation is affected by both wind-driven gyres through their western boundary currents and wind-stress forcing on the shelf especially along the coasts of Newfoundland and Labrador. The local wind stress forcing has more direct impacts on flows in shallower waters along the coast while the open-ocean gyres tend to affect the circulations along the outer shelf. Our conclusion is that wind stress is an important forcing of the main along-shelf flows in the NWA. One objective of this study is to motivate further examination of whether wind stress is as important as freshwater forcing for the mean flow.

Plain Language Summary Between Greenland's southern coast and Cape Hatteras there exists a continuous and equatorward flow shoreward of the shelf break. The prevailing understanding is that this coastal flow system is maintained by freshwater discharges from rivers and glaciers while wind stress is important for its variability. The role of wind stress for the mean flow has not been adequately studied. In this study, we use a 2-layer model that is forced by wind stress alone and show that the wind stress drives a shelf circulation system that is similar to what has been characterized by observations. Our numerical simulations indicate that the wind stress forcing is likely to be as important as buoyancy forcing for both the mean flow and its seasonal variability. A main objective of this work is to motivate further studies to examine and quantify the relative contributions from wind and freshwater discharge to the mean transport and its variability, and to investigate the interactions between wind-driven and freshwater-driven processes.

1. Introduction

The circulation over the continental shelf in the Northwest Atlantic (NWA) is characterized by equatorward flows from Greenland's southern coast to Cape Hatteras (Figure 1). Based on hydrographic and isotopic analyses, Chapman and Beardsley (1989) postulated that the NWA coastal currents north of Cape Hatteras are one continuous circulation system that is driven predominantly by buoyancy fluxes from freshwater discharges from the rivers and glaciers along the coast. This concept has been broadly accepted based on the interpretations of model simulations and observations, many of which focus on the Mid-Atlantic Bight (MAB) where more observations are available. For the depth-integrated mean flow, the along-shelf momentum balance is mainly between along-isobath components of wind stress, sea-level gradient and bottom friction (Csanady, 1976). Because the local wind stress is weak between Cape Hatteras and Nova Scotia, the momentum balance there is mainly between the bottom drag and along-shelf sea-level gradient (Lentz, 2008a). It was Stommel and Leetmaa (1972) who first recognized that an along-shelf sea-level gradient, which they estimated to be on the order of 10^{-7}, must exist to sustain the mean flow in the MAB. Scott and Csanady (1976) estimated the sea-level slope to be about 1.4×10^{-7} over the inner shelf off Long

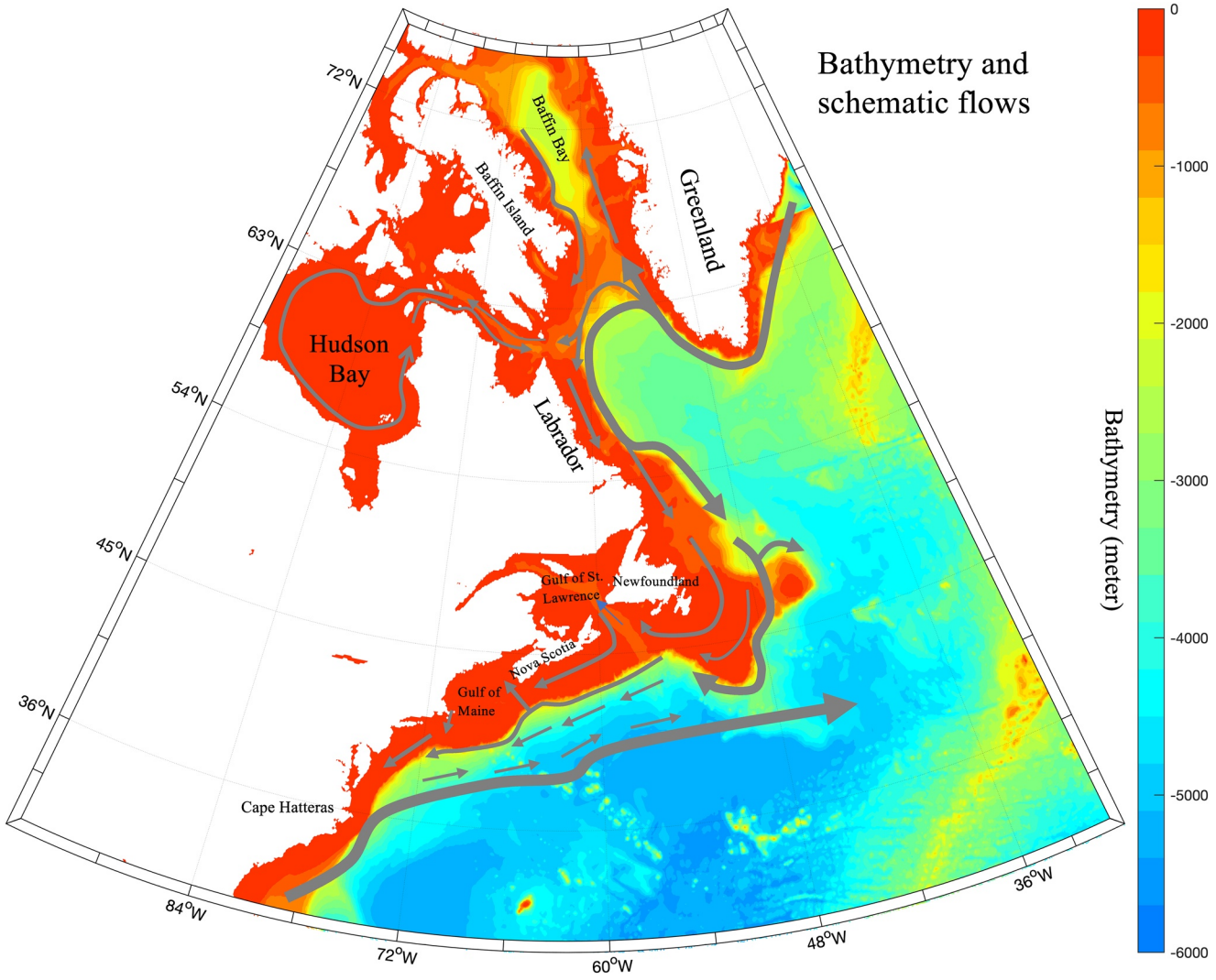

Figure 1. Schematic diagram of the circulation features in the NW Atlantic coastal ocean (after Townsend et al., 2015 and Saucier et al., 2004). The background color is the bathymetry (meters).

Island. More recently, Lentz (2008a) revised the gradient to be around 3.7×10^{-8} based on the depth-averaged momentum balance in the MAB but reaffirmed that it is the dominant term in the momentum budget driving the mean along-shelf flow. Since the mean flow in the MAB is maintained mainly by the along-shelf sea-level gradient, the forcing of the flow, therefore, may be traced at the origins of sea-level gradient, which are not necessarily in the MAB (e.g., Pringle, 2018; Xu & Oey, 2011).

An origin of the along-shelf pressure gradient in the MAB, according to Pringle (2018), is the freshwater runoff from St. Lawrence River. The forcing would affect circulation only in the downwave (which is equatorward in the NWA) region (Csanady, 1985; Vennell & Malanotte-Rizzoli, 1987). If the same model is applied to each freshwater source along the NWA coastline, the collected effect would be a sustained equatorward coastal flow that is locally boosted by each freshwater source. Xu and Oey (2011) found that the MAB circulation in their model is mainly forced by the open boundary condition from the coast to 1,000 m isobaths of Scotian Shelf without specifically identifying the origin of the pressure gradient. Their study, however, did show that the cross-slope/shelf influence from the deep ocean gyres, if exists, must occur in the upstream regions, not within the MAB segment.

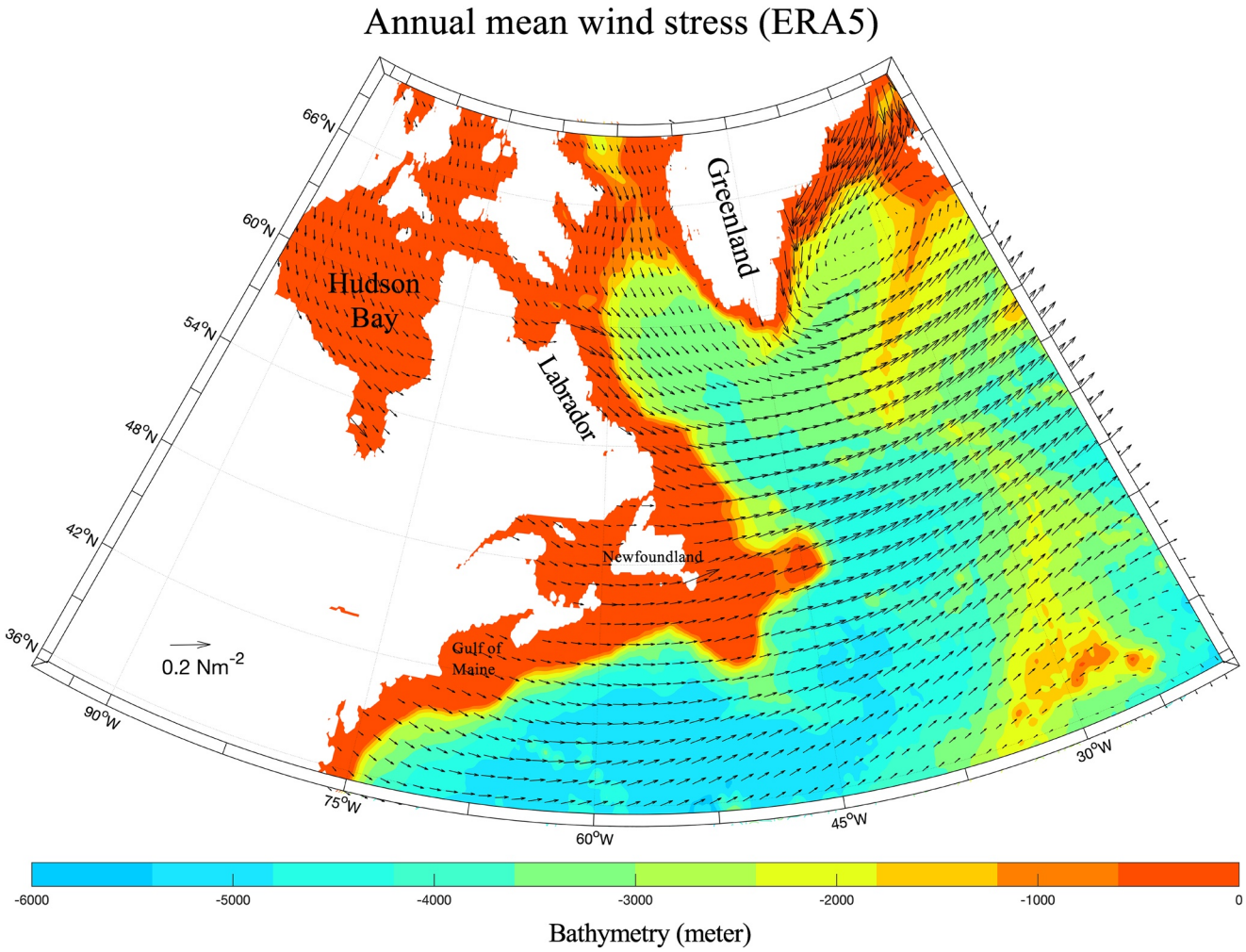

Figure 2. The annual-mean wind stress climatology from ERA in the NWA region. Note that the wind stress in the NWA shelves is weak south of Newfoundland but it is very strong in the subpolar region, especially along the coast of Labrador. It is shown in this study that this strong equatorward wind stress along the coast is a main source for the along-shelf sea-level gradient that maintains the mean flow on shelves in the downwave direction all the way to Cape Hatteras. The background color is the bathymetry (meters).

While wind stress forcing is known to be important for seasonal variability of Labrador and Newfoundland shelf flows (e.g., Han et al., 2008; Wang et al., 2015 for model and data syntheses), it has not been adequately investigated as a main driver for the mean flow over the entire NWA shelf. The wind stress is weak and against the mean flow in the MAB and Scotian shelves (Lentz, 2008a). However, north of Newfoundland the wind is strong and mostly in the same direction as the mean flow (i.e., equatorward) (Figure 2). This would favor an onshore convergence of the Ekman transport and possibly lead to an elevated sea level near the coast. Does wind stress there play a role as important as the buoyancy forcing for the mean coastal flow on the Labrador shelf? If so, does the wind forcing on the Labrador shelf and further north remotely influence the mean circulation downstream on the Scotian Shelf and in the MAB? These are among the questions that we aim to explore in this study.

The cross-shelf forcing from large-scale open-ocean processes, such as wind-driven gyres, is another potentially important mechanism for influencing the along-shelf mean flow (Beardsley & Winant, 1979; Csanady, 1976). However, Wang (1982) and Chapman (1986) demonstrated that the topographic barrier would effectively block open-ocean forcing from crossing the shelf break to influence the MAB mean flow in idealized barotropic models. Interestingly, the cross-shelf open-ocean forcing has been widely accepted as the leading mechanism for sustaining a northward warm current in the Northwest (NW) Pacific marginal seas from the South China Sea to Japan Sea against the prevailing southwestward annual mean wind stress

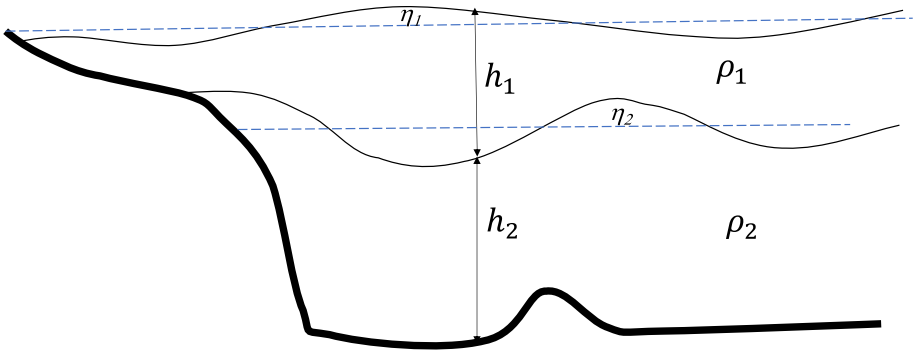

Figure 3. Schematic of the two-layer model. The model uses ETOP 5 bathymetry and is forced by ERA Interlim monthly climatologic wind stress. The minimum water depth is 5 m.

(e.g., Ma et al., 2010). The dynamical settings between the NW Atlantic and NW Pacific are similar, both bordering major western boundary currents. It is intriguing to ask whether the open-ocean processes play a similarly important role in forcing the mean flow and the variability on the NWA shelf when realistic bathymetry and forcings are considered. This deep-ocean forcing mechanism will be examined in our study using a two-layer model with a realistic topography, which is perhaps the simplest possible model for the purpose of our study. The cross-shelf exchanges are strongly affected by bathymetric features that vary greatly along the NWA shelf. It would be necessary to use a realistic topography so that areas of enhanced exchanges can be identified and related bathymetry features. The second consideration is that the cross-shelf gradient of potential vorticity (PV) $q = f/h$ (where h is the layer thickness) may be unrealistically large in barotropic models because the wind-driven gyres in the open ocean are confined mostly in the upper layer above the thermocline where $h \sim$ 1,000m instead of $h \sim$ 5,000m in barotropic models. The rationale of this approach is to have a good understanding of the fundamental dynamics in a relatively simple setting before using more complex three-dimendional primitive equation models.

The study is organized as follows. The detail and the setup of the two-layer wind-driven model is described in next section. This will be followed by presentation and discussion of Control Run results. In section 4, we present and discuss results from a number of sensitivity tests aiming to examine the role of wind stress forcing in various shelf regions and the influence from open ocean processes. Further discussion will be made and a summary will be provided in Section 5.

2. Model

The main objective of this study is to examine whether wind-stress forcing is important for the mean flows on the NWA shelves, which have been attributed mainly to buoyancy forcing in previous studies. Therefore, we conduct model experiments using wind-stress forcing only. Surface buoyancy fluxes and river runoffs are excluded in the forcing fields. The two-layer primitive equation model, described by Yang (2015), have both layers active so that it includes the barotropic and first baroclinic modes (Figure 3). The model is adiabatic, meaning no exchanges of water masses between two layers, and is driven by wind stress only. The model is governed by the following equations.

$$\frac{\partial \vec{u}_1}{\partial t} + \vec{u}_1 \cdot \nabla \vec{u}_1 + f\vec{k} \times \vec{u}_1 = -\frac{1}{\rho_0}\nabla p_1 + \frac{\vec{\tau}}{\rho_0 h_1} z + A\nabla^2 \vec{u}_1 + \vec{F}_1, \tag{1a}$$

$$\frac{\partial \vec{u}_2}{\partial t} + \vec{u}_2 \cdot \nabla \vec{u}_2 + f\vec{k} \times \vec{u}_2 = -\frac{1}{\rho_0}\nabla p_2 + A\nabla^2 \vec{u}_2 + \vec{F}_2, \tag{1b}$$

$$\frac{\partial h_1}{\partial t} + \nabla \cdot \left(h_1 \vec{u}_1\right) = 0, \tag{1c}$$

$$\frac{\partial h_2}{\partial t} + \nabla \cdot \left(h_2 \vec{u}_2\right) = 0. \tag{1d}$$

where the pressure gradients are related to sea surface height η_1 and height of layer interface η_2 (see Figure 3 for model schematic):

$$\frac{1}{\rho_0}\nabla p_1 = g\nabla\eta_1 \text{ and } \frac{1}{\rho_0}\nabla p_2 = g\nabla\eta_1 + \frac{(\rho_2 - \rho_1)}{\rho_0} g\nabla\eta_2. \quad (2)$$

The last terms in Equations 1a and 1b, that is, $\vec{F}_n$, represent the bottom drag. For the upper layer the bottom drag $\vec{F}_1$ is applied only when the layer is in contact with bottom, that is, when $h_2 = 0$. The bottom drag is computed by using a quadratic form, that is, $\vec{F}_n = C_d\vec{u}_n|\vec{u}_n| / h_n$. In most of our simulations we use $C_d = 1\times10^{-3}$, a value that is estimated by Lentz (2008a) in the MAB area. We have conducted several sensitivity tests by varying the value of this drag coefficient and found that the overall circulation pattern remains the same but the magnitude of the along-shelf sea-level gradient and the velocity decrease when a larger C_d is used. For example, the mean sea-level gradient between Labrador shelf and MAB would decrease by about 25% if C_d is increased from 1×10^{-3} to 5×10^{-3}. More detail about this sensitivity will be presented and discussed in next section. We use $A = 500\ \text{m}^2\ \text{s}^{-1}$ for the lateral viscosity, accounting for the unresolved sub-grid scale mixing. The width of the Munk boundary, $L_M \sim (A/\beta)^{1/3}$, is about 35–50 km for the subtropical and subpolar gyres, which is resolved by 3–4 model grids. In general, using a greater viscosity A tends to weaken velocity over the whole model domain. The flow on the shelves, however, is considerably more sensitive to the bottom drag than the lateral viscosity A. The density difference is set to be $\Delta\rho = \rho_2 - \rho_1 = 1\text{kg m}^{-3}$.

The model domain extends from 20°S to 80°N meridionally and from 100°W to 20°E zonally and has a spatial resolution of 1/8°. The model is discretized on an Arakawa C-grid. The lateral boundaries are all closed. The model is fully nonlinear and allows the thickness of either layer to become zero (i.e., outcropping of lower layer and grounding of the upper layer). The model's initial condition is the state of rest and the initial layer interface is set at 800 m depth. Most shelf regions are covered by the upper layer only and so the governing dynamics are intrinsically barotropic. The model is forced by wind stress from ERA-Interim and uses the ETOPO5 bathymetry (the minimum water depth in the model is set at 5 m) (Figure 1). The monthly wind stress climatology is interpolated linearly to each time step, which is $\Delta t = 10$ s. Synoptic scale forcings, such as storms, are typically filtered out in long-term climatology data. A small time-step Δt is used to ensure the numerical stability because the model explicitly resolve fast barotropic waves.

The ocean's spin-up time scale, as explained by Anderson and Gill (1975), is set by the basin-crossing time scale of long baroclinic Rossby waves from the eastern to western boundaries. The planetary Rossby waves are slow due to a small gradient of planetary vorticity, that is, β, in high latitudes. Assuming that the internal deformation radius of 15 km in 60°N, linear long Rossby waves propagate about 100 km per year and would take about 50 years to cross a basin of 5,000 km wide. This is consistent with our model spin-up time scale of about 40–50 years to reach a steady seasonal cycle. In this study we run each experiment 100 years by repeating the annual climatological forcing.

Surface wind stress from ERA-Interim covers both ocean and land. There is a large change of surface stress across the land-sea boundary, with stress in land grids typically a factor of 2–3 greater than that in the neighboring sea grids. The difference is mainly due to the surface roughness. The land mask file from ERA-Interim provides information about the percentages of land and sea for those grids along the coast. To avoid unrealistic wind stress in those coastal sea grids with partial land coverages, we use averaged stress from the neighboring sea grids within a 50 km radius. We have also tested an alternative method by simply setting any partial land grids to completely land-filled grids. The results are similar to that from the first method.

3. Results

The aforementioned model is integrated for 100 years to reach the steady state. The daily output (at the last time step on each day) of model variables in the 100 year result is used in the following analyses. The annual-mean sea surface height (SSH, Figure 4) shows a typical pattern of subtropical and subpolar gyres. The annual-mean transport of Gulf Stream at 30°N is about 30 Sv with the SSH difference of about 30 cm

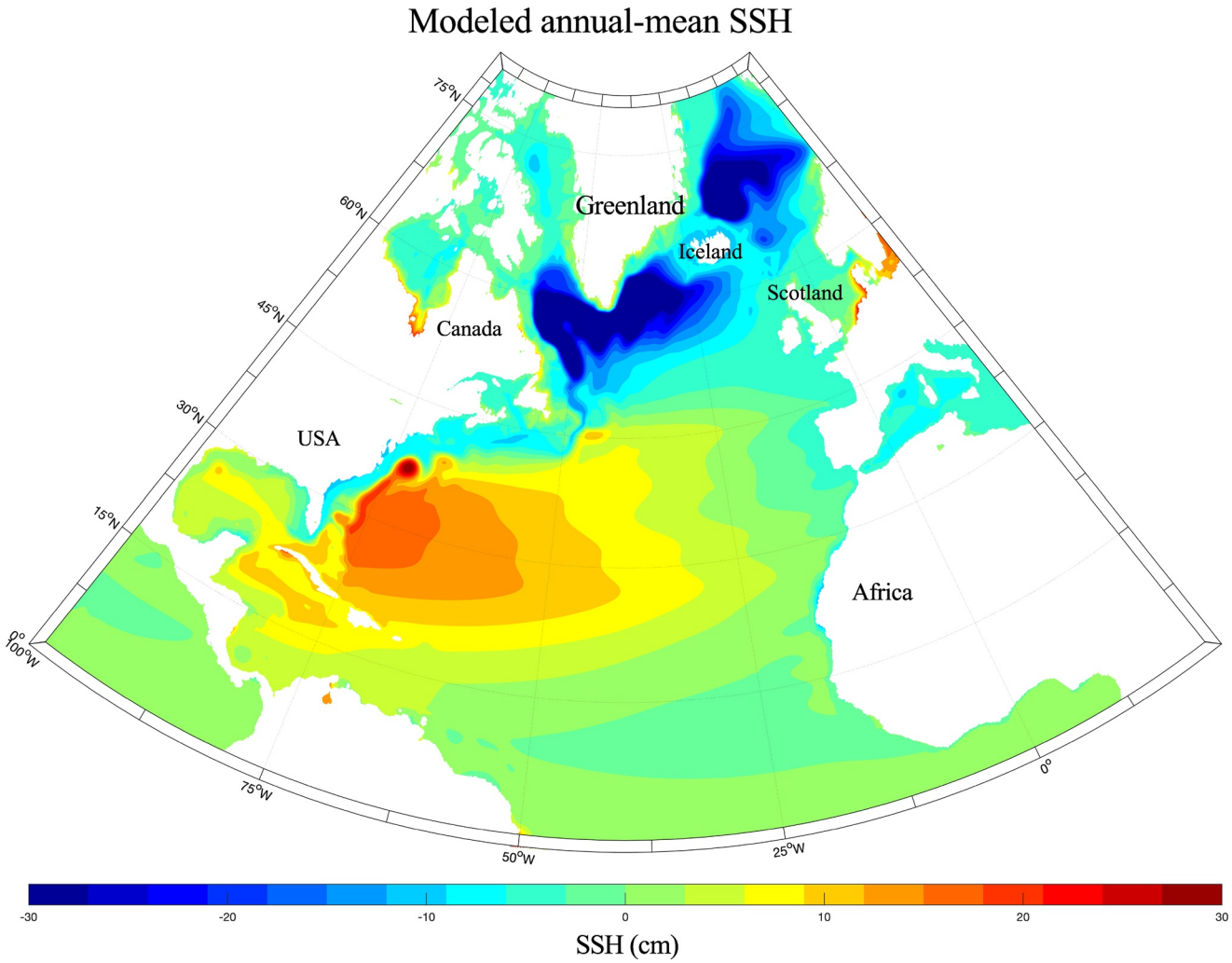

Figure 4. The annual-mean sea surface height from the Control Run (unit: cm).

across the stream. There is a large anti-cyclonic eddy or localized recirculation associated with the Gulf Stream separation from the western boundary. The northern edge of this eddy is about 37°N–38°N, which is about 2° further north of Cape Hatteras where the Gulf Stream actually separates from the shelf. This northward bias of Gulf Stream separation, as we will discuss later, affects the shelf and slope circulations in the MAB region (see Chassignet and Marshall, 2013 for a review of common biases in numerical models). The subpolar gyre is separated to two sub-gyres north and south of the Greenland-Iceland-Scotland Ridge (GISR). The two cyclonic gyres are connected by a northward flow across the GISR between Iceland and Scotland and a south East Greenland Current through Denmark Strait. These are consistent with observed features as reviewed by Dickson et al. (2008).

This study focuses on the shelf circulation in the NWA. Therefore, we present analyses mainly in the NWA region in the remaining of this study. The results for some other regions from the same model have been described in previous publications (e.g., Yang & Pratt, 2013, 2014; Yang, 2015). We will first discuss the annual mean fields, followed by some discussions of the seasonal variability. The roles of deep-ocean influence and wind stress forcing on shelves will also be examined.

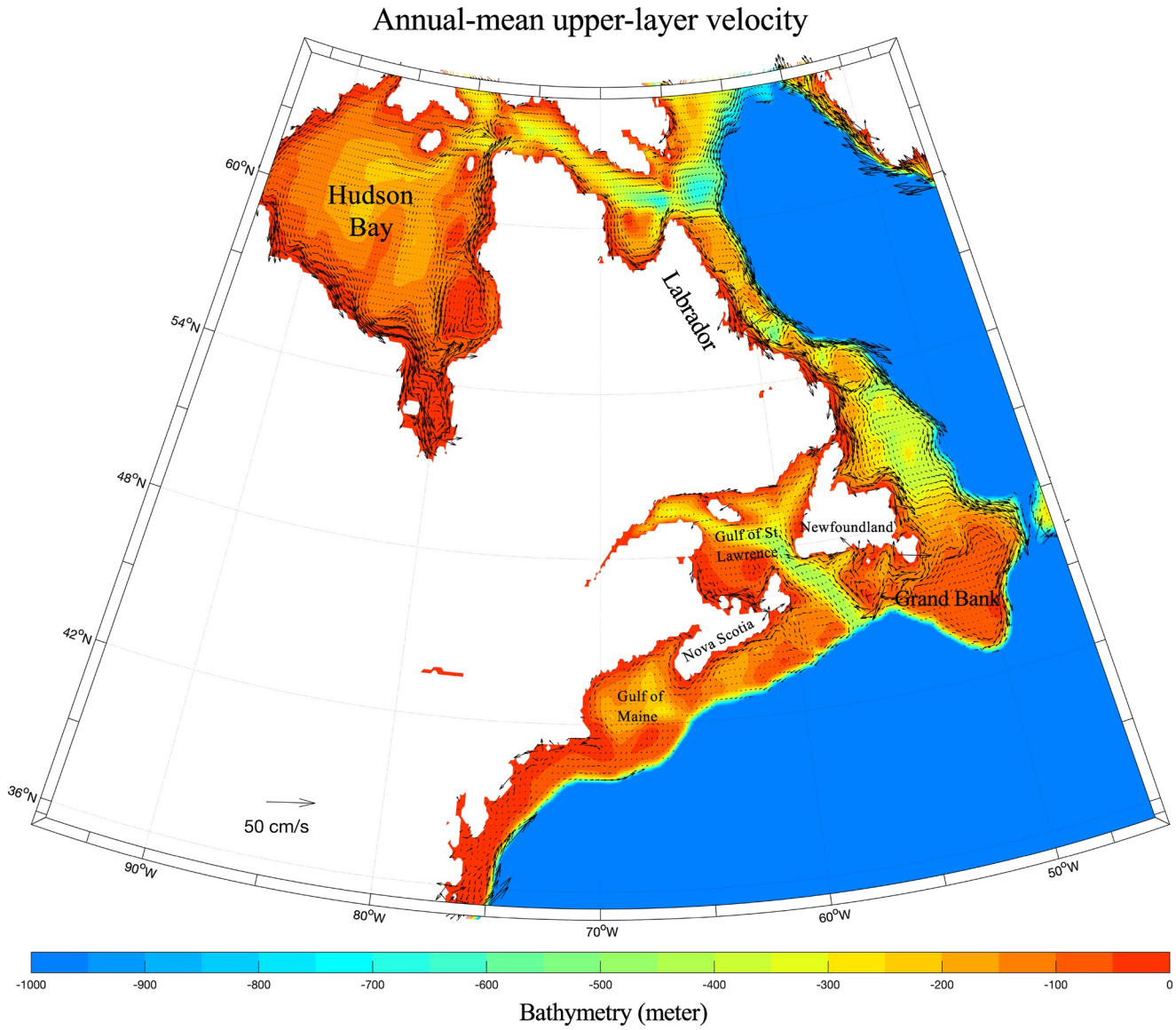

Figure 5. The annual-mean velocity (vectors) on shallow areas where the water depth is shallower than 1,000 m (the velocity vectors and bathymetry in deeper areas are excluded in this plot to avoid visual distraction from flows on shelves and slope). The background color represents the bathymetry (unit: meter).

3.1. Annual Mean Along-Shelf Flows:

The modeled annual-mean shelf circulation (Figure 5) is broadly consistent with the observation-based description (Figure 1), including all key regions except the area just off the Cape Hatteras where the shelf circulation was influenced by a northward shift of the Gulf Stream separation, a common problem in numerical models (e.g., Chassignet & Marshall, 2013). From the MAB to Scotian shelves the velocity is in the range of 1–10 cm s^{-1} between the coast and 150 m isobath, consistent with the long-term observations described by Lentz (2008a). The southwestward along-shelf velocity across 60°W off Nova Scotia, for instance, increases from 0 at boundary to about 6.5 cm/s at 140 m depth (Figures 5 and 10). The flow at the outer shelf in the MAB is affected by the northward bias of the Gulf Stream separation and thus the unrealistic representation of shelf-slope density gradient in the model. For example, the flow across 71°W is equatorward with the westward velocity reaches the maximum of about 3.5 cm/s at 90 m depth, and then decreases seaward to 2.86 cm/s at 130 m depth. The flow reverses the direction to eastward at about 400 m depth. This indicates a considerable influence of open-ocean processes on shelf flows. The along-shelf velocity is much stronger along the coast of Newfoundland and Labrador. Across 52°N just north of Newfoundland, the

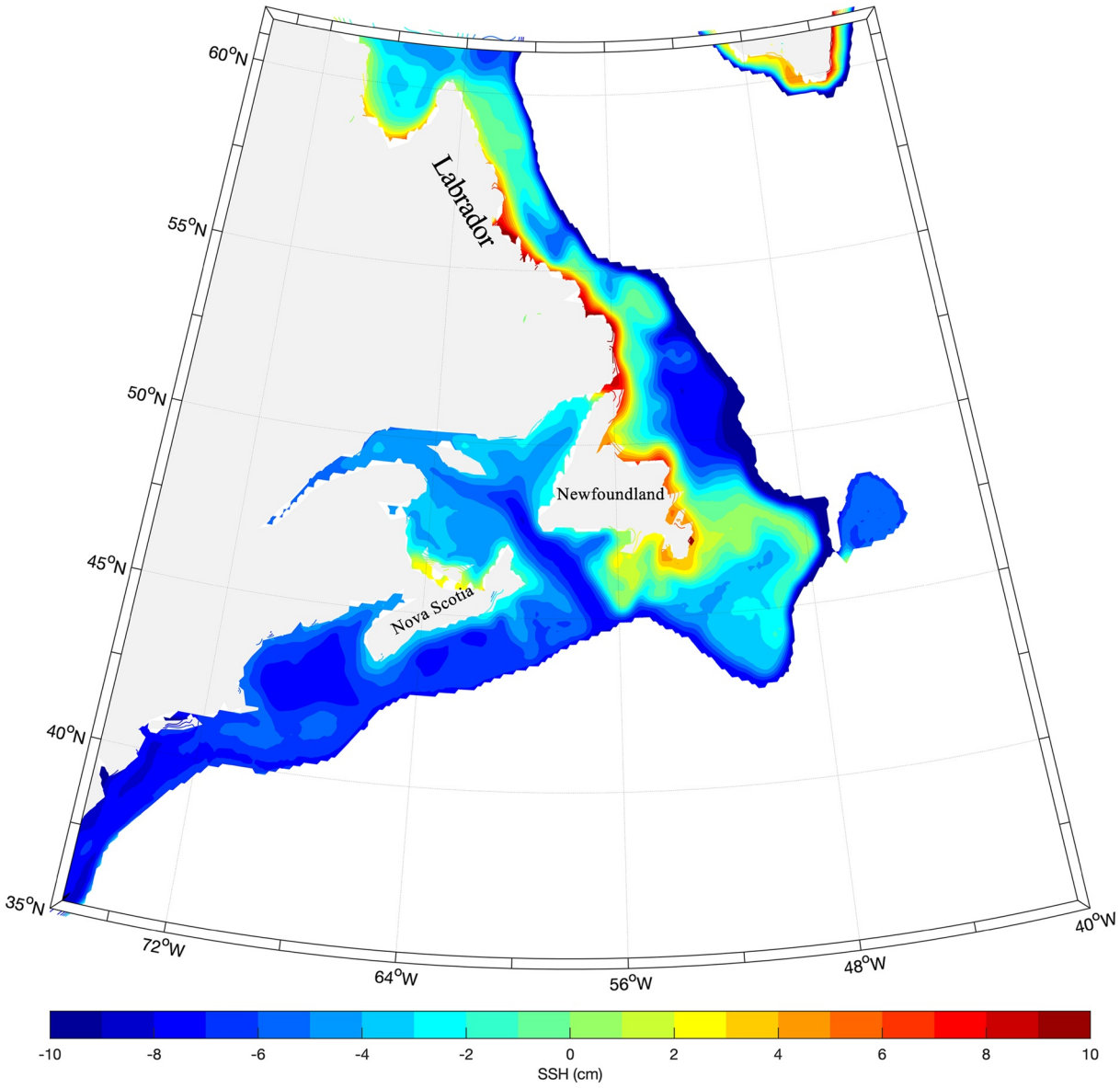

Figure 6. The annual-mean sea surface height, the same model variable plotted in Figure 4, in the NWA region where the water depth is shallower than 1,000 m. The SSH is not shown (white color) wherever the water depth is greater than 1,000 m for better visualization.

equatorward velocity increases from 0 at the boundary (due to no-slip condition) to about 20 cm/s at 115 m isobath with an annual mean transport of 1 Sv between the coast and 200 m depth (Figure 9).

The along-shelf sea-level gradient is important in maintaining the equatorward shelf flow in the NWA (Csanady & Scott 1976; Lentz, 2008a; Stommel & Leetmaa, 1972). The annual-mean sea surface height along the coast from Greenland to Cape Hatteras has three areas of pronounced high SSH: the southeast Greenland's coast, the southern boundary in Hudson Bay and the coast of Labrador (Figure 6). The wind stress pattern in these three regions are similar that the wind is strongly along-shelf and favors an onshore Ekman transport. For example, the wind stress between Denmark Strait and Cape Farewell in the southern tip of Greenland is strongly southwestward along the coast. The Ekman convergence would result in a "pile up" of surface water and elevates the SSH at the coast. The locally elevated SSH would fade in the downwave direction (Csanady, 1985; Vennell & Malanotte-Rizzoli, 1987). Both boundary Kelvin waves and topographic Rossby waves propagate in the equatorward direction along the NWA region, so the high SSH

would decrease gradually in that direction due to friction. The SSH on the southwest coast of Greenland, which is in the downwave region from the east Greenland coast, still remains relatively high even though the local wind stress there forces an offshore Ekman transport. The decay length scale in the along-shelf direction is mainly controlled by the bottom drag coefficient (Csanady, 1978). This downwave spread of sea level is also referred to as "arrested topographic waves" (Csanady, 1978, 1982).

Another area of pronounced high SSH is along Labrador Sea's boundary between 50°N and 60°N. This heightened SSH, like the one alone Greenland coast, extends equatorward in the downwave direction to Newfoundland's coast. As we will discuss further, this sea-level gradient that is originated in Labrador coast is particularly influential for the mean flow as far away as in the Gulf of Maine and MAB. Farther upstream inside the Hudson Bay the sea level is high along the southern boundary. The annual-mean wind stress inside the Bay, though not as strong as that along the southeast Greenland coast or along the Labrador coast, is southeastward (Figure 2). This forces a southward convergence of Ekman transport and result in high SSH along its southern boundary. This high SSH affects the boundary currents inside Hudson Bay and outflow along Hudson Channel. But it's impact on downstream shelf flows outside the Bay, such as in Newfoundland shelves, is diminished by bottom drag over a decay length scale of arrested topographic waves (Csanady, 1978). In the model, we use the quadratic bottom drag and so the decay scale can be estimated by assuming the balance between along-shelf pressure gradient and bottom drag:

$$-g\frac{\partial \eta}{\partial l} \sim -C_d\frac{|v|v}{h}, \tag{3}$$

where the pressure gradient is in the along-isobath direction, and h is the water depth. Assuming $\Delta\eta \sim 0.1\,\mathrm{m}$, $\mathrm{v} \sim 0.15\,\mathrm{ms}^{-1}$ and $h \sim 50\mathrm{m}$, the length scale is approximated:

$$L \sim \frac{hg\Delta\eta}{C_d v^2} \sim 2\times 10^3\,\mathrm{km}$$

The estimate is rough and highly sensitive to water depth h and the drag coefficient, which is 10^{-3} in the model.

This study focuses on the mean shelf flow from Labrador coast to the MAB and the analyses presented in following will be centered on this region. To evaluate the mean along-shelf pressure gradient in this region we computed the averaged SSH between the coast and 150 m isobaths along the coast from 56°N to 38°N (black line in Figure 7). Overall, the sea level decreases equatorward in this region. The most rapid change occurs between the Newfoundland and Nova Scotia. In the MAB the difference of sea level between 41°N and 37°N is 1.7 cm, yielding an averaged slope of sea level about 3×10^{-8} to 4×10^{-8}. This sea-level slope compares remarkably well with the observation-based estimate of 3.7×10^{-8} obtained by Lentz (2008a). The sea-level gradient in the model is sensitive only to the bottom quadratic drag coefficient, which is set to be $C_d = 1\times10^{-3}$. This is the same value estimated by Lenz (2008a) at 5 m above the bottom in the MAB. We tested the model sensitivity by varying C_d between 1×10^{-3} and 5×10^{-3} and found the overall pattern is similar (Figure 8). The sea-level slope from Labrador shelf to MAB decreases by about 25% when C_d is increased from 1×10^{-3} to 5×10^{-3}. The velocity field (not shown) is also similar qualitatively to that from control run but weaker in velocity amplitude when a greater C_d is used. It is interesting to note that the sea level is more sensitive to C_d on Labrador shelves than in the MAB (Figure 8). This is likely due to the fact that the mean along-shelf velocity is much stronger in subpolar latitudes and thus the quadratic bottom friction is more sensitive to changes in C_d.

To better describe the shelf transport in the wind-driven model, we compute the transport of the along-shelf flow starting at the Baffin Island's coast. These transports represent the sole contribution of wind stress, and the numbers reported below should be interpreted with this in mind. Figure 9 shows the transport between the coast and 200 m isobath (except for Hudson Strait and Laurentian Channel where the total transports across all depth are computed). For each section, we present the transports for the annual mean, June and December. To the north of Hudson Strait the flow is southward along Baffin Island's coast (Figures 1 and 5). The annual mean transport between the coast and 200 m isobath is about 0.18 Sv (Figure 9). The

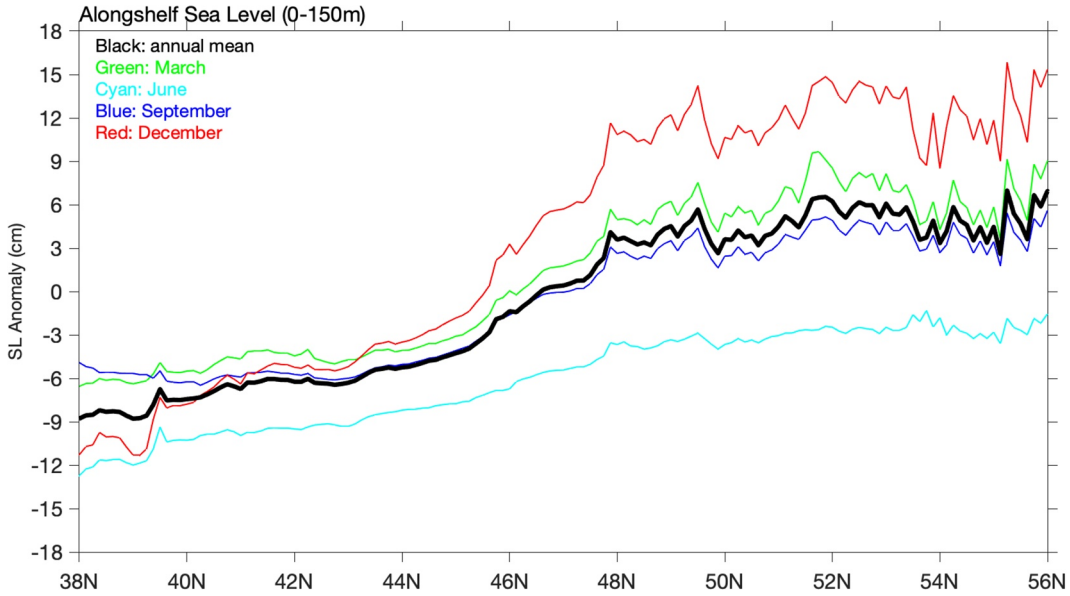

Figure 7. Average sea-level between the coast and 150 m isobath for the annual mean (thick black line), March (green), June (cyan), September (blue), and December (red). The sea-level slope is greatest in late fall and weakest in late spring and early summer. This seasonal cycle is consistent with a data-assimilative model and observations. The large change of sea-level gradient between 44°N and 48°N is due the existence of St. Lawrence Channel.

annual mean circulation is cyclonic inside the Hudson Bay (Figure 5), which is consistent with previous studies (e.g., Saucier et al., 2004). There is a westward inflow along the northern Hudson Strait, which is a continuous coastal flow from Baffin Island's coast. On the southern side of the strait there is an exit flow from the Bay. The annual mean of exchange flow transport is 0.32 Sv. It should be noted that the inflow/outflow transport here includes flows at all depth. The transport for the inflow between 0 and 200 m isobath is only about 0.15 Sv, which is more comparable with 0.18 Sv off Baffin Island's coast. Along Labrador's

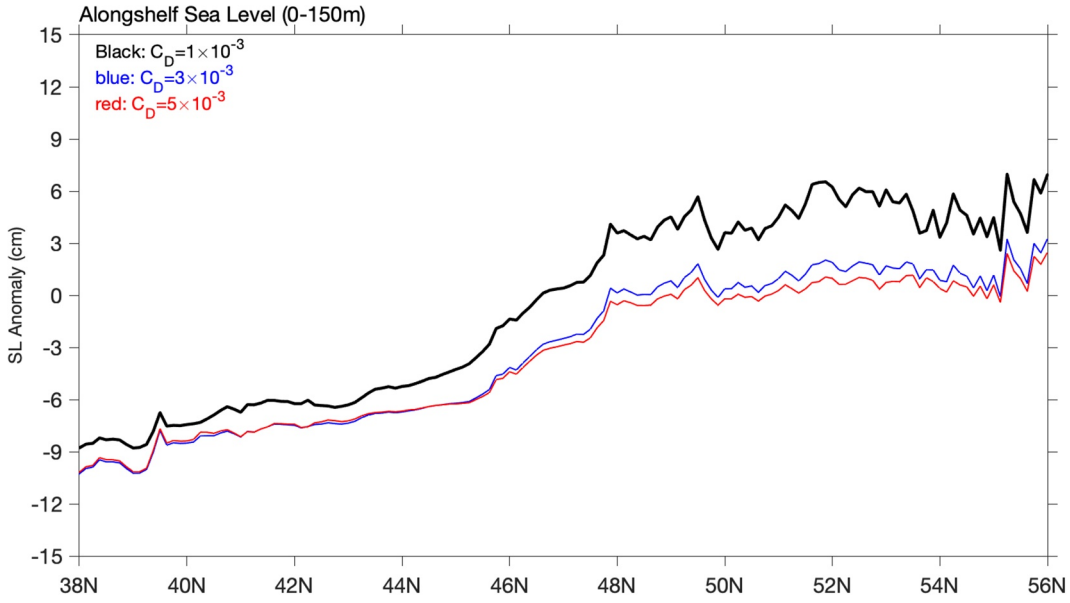

Figure 8. Sensitivity of the along-shelf sea-level gradient to bottom drag coefficient. The control run uses $C_D = 1 \times 10^{-3}$, a value estimated by Lentz (2008a). When the drag coefficient increases the sea-level gradient decreases accordingly. The sea-level gradient decreases about 25% when $C_D = 5 \times 10^{-3}$ is used.

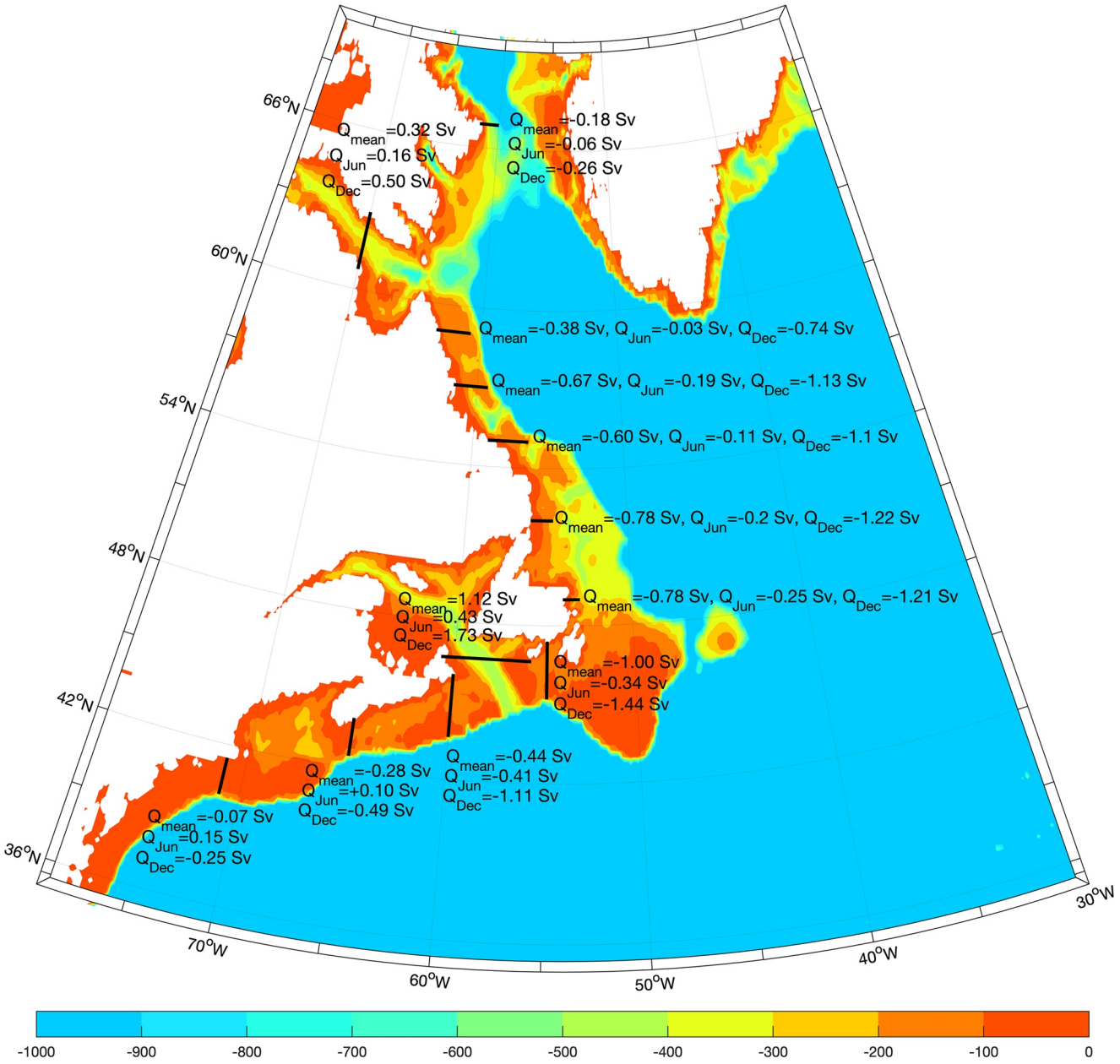

Figure 9. Volume transports between the coast and 200 m isobath (except Laurentian Channel and Hudson Strait, where the transport is total across all depth) along the NWA coast from the Control Run. The background color is the bathymetry (meters).

coast the annual-mean transport between 0 and 200 m isobath increases from 0.38 Sv at 59°N, which is just the downstream of the Hudson Strait, to 0.67 Sv at 57°N. It remains relatively unchanged, between 0.60 and 0.78 Sv, all the way to 49°N off Newfoundland's coast. The mean transport increases over the Newfoundland shelves to 1 Sv at 55°W. There is an inflow into the St. Lawrence Gulf along northern Laurentian Channel and an outflow of the equal transport along the southern part of the channel. The transport of the inflow or outflow across Laurentian Channel is 1.12 Sv. The southeastward outflow from Gulf of St. Lawrence turns southward along coast of Nova Scotia (Figure 5). The transport between 0 and 200 m isobath is 0.44 Sv at 60°W. The transport weakens as it continues southward and is reduced to 0.28 Sv at 65°W just upstream to Gulf of Maine. The flow in Gulf of Maine (GoM) is cyclonically along the boundary. The coastal flow continues southward after exiting from GoM. The transport becomes very small, less than 0.1 Sv at 71°W just south of Cape Cod.

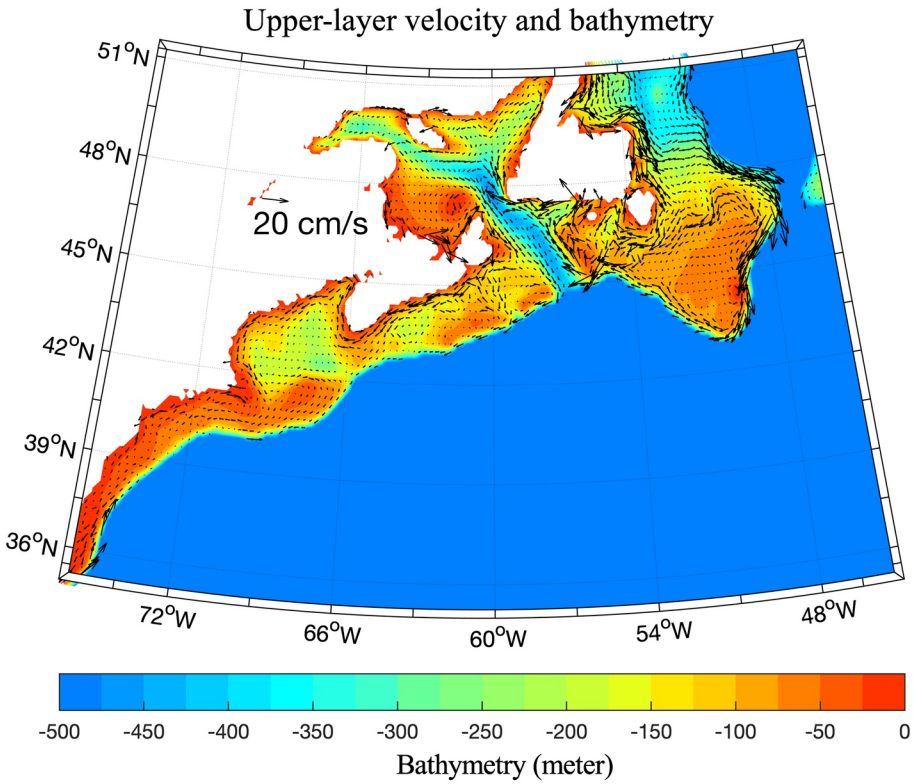

Figure 10. The annual-mean velocity between the coast and 500 m isobath from the control run. (The background color is bathymetry, unit: meter).

The transport of the shelf flow in the MAB between the coast and 200 m is rather weak. The flow between 75°W and 70°W, for instance, is mostly southward between the coast and 125 m isobath (Figure 10). However, along-isobath flow turns northward in shelf break deeper than 125 m. This northward flow is associated with the Gulf Stream, which separates from the coast about 2° north of Cape Hatteras. The northward bias in Gulf Stream separation is one of the most common problems in numerical models. It has been attributed to various causes, including model resolution, bathymetry, interactions with deep western boundary currents, etc.

3.2. Seasonal Variability

Surface wind stress varies significantly with seasons in the NWA region (Figure 11). In summer it is particularly weak along the coast of Labrador and Newfoundland. To the south of Newfoundland on Scotian shelves, Gulf of Maine and in MAB, the wind stress in June is parallel to the coast and is dominated by southwesterly against the equatorward mean flow. This is in contrast to the annual-mean field (Figure 2) in which the wind is mainly northwesterly and is perpendicular to the coastline in these regions. The wind stress in Hudson Bay and along Hudson Strait is weak in June. It is interesting to note that the annual-mean wind stress in Laurentian Channel is in the along channel direction toward the open Atlantic Ocean (Figure 2). The wind in June, however, is blowing northeastward across Laurentian Channel. The wind stress in December (right panel, Figure 11) is much stronger than both the annual-mean field and that in June. The wind direction in each region is very similar to that in the annual-mean wind stress, indicating that the annual-mean wind stress is largely determined by the strong wind field in fall and winter.

In response to the wind forcing, the shelf circulation varies seasonally. The equatorward transport on the Labrador and Newfoundland shelf, for instance, is strongest in late fall and weakest in late spring and early summer, consistent with observations and modeling results (Han et al., 2008; Hannah et al., 2001; Lazier & Wright, 1993; Saucier et al., 2004; Wang et al., 2015; Wu et al., 2012). The large seasonal changes in

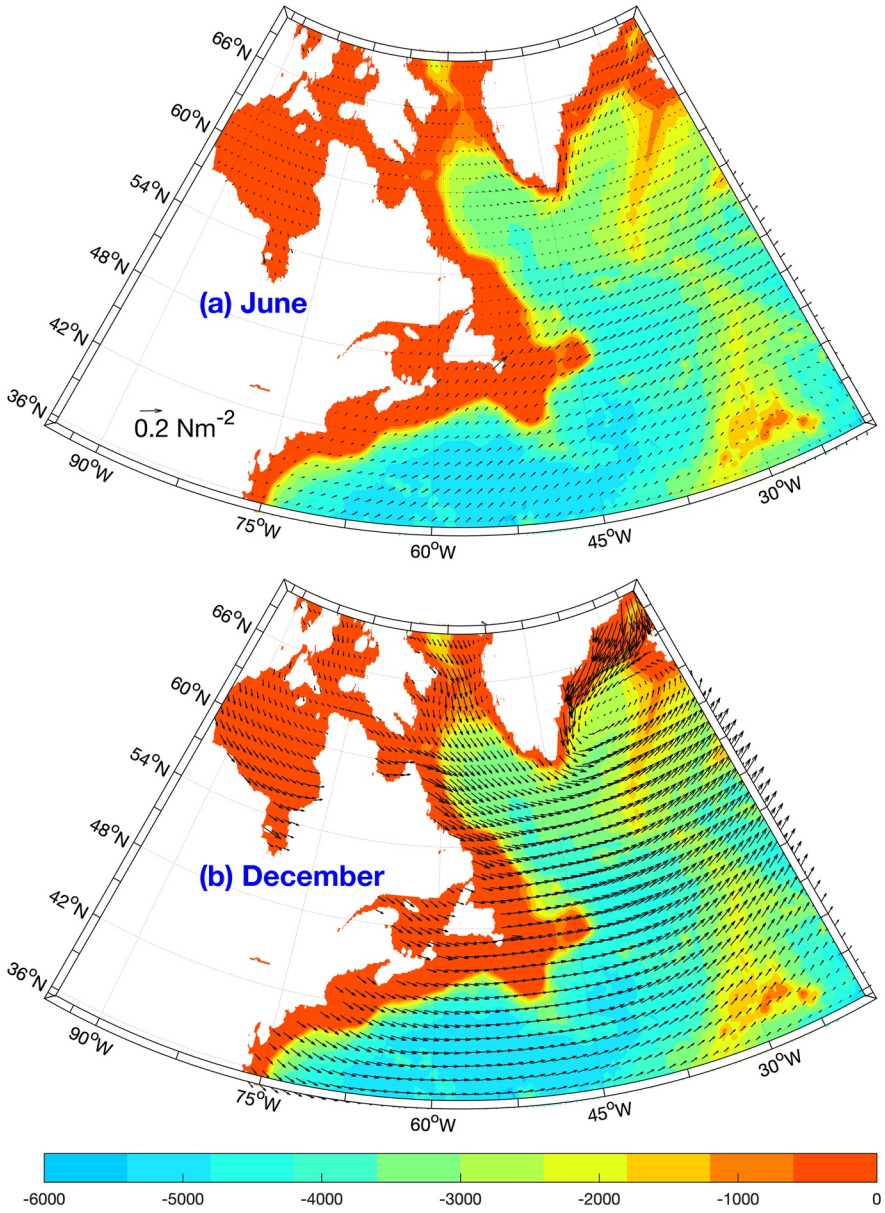

Figure 11. Wind stress (vectors) and bathymetry (background color, unit: meter) in June and December, the two months where the along-shelf flow has the minimum and maximum transport.

along-shelf current transport are clearly revealed in Figure 9. The transport between 0 and 200 m isobath is typically much larger in December than in June along the entire NWA coast between from Greenland coast to the MAB. For instance, the equatorward transport along Labrador and Newfoundland's coast is only about 0.1–0.25 Sv in June, but is typically over 1 Sv in December. The transport of inflow/outflow along Laurentian Channel increases from 0.43 Sv in June to 1.73 Sv in December. The large seasonal variability is also shown for shelf flows on the Scotian shelf, in the Gulf of Maine and on the MAB shelf.

The seasonal variability of the along-shelf flow is related to seasonal changes in sea level. In our model, the sea level at St. Johns, for instance, varies about 18 cm between the seasonal high in December and low in June. This is almost identical to the tide gauge observation and a data-assimilative model result reported by Han et al. (2008). Lazier and Wright (1993) attributed the seasonal variability of Labrador current to a seasonal change of sea level of about 12 cm on the shelf. They further attributed this seasonal change to the change of buoyancy of the shelf water (steric effect). It is interesting to note that the sea-level difference

between December and June in this wind-driven two-layer model is about 10–15 cm on the Labrador shelf (Figure 7), indicating that the wind forcing is probably at least as important as the buoyancy forcing in this region. Some discrepancies, however, do exist. The velocity measured at 200, 400 and 985 m isobaths at the Labrador shelf/slope in the 1970s and 1980s reaches minimum in April and maximum in November (Lazier & Wright, 1993). Our model result shows about a one-month delay in the seasonal cycle, that is, minimum in May and maximum in December (not shown). The discrepancy may reflect the interaction of buoyancy forcing and wind stress, and will be investigated in future studies.

Figure 7 shows the averaged sea level between 0 and 150 m isobath along the coast from 38°N to 56°N for the annual mean (black), March (green), June (cyan), September(blue), and December (red). The largest seasonal changes occur north of 45°N along the coast of Labrador and Newfoundland where the difference between June and December is as large as 15 cm. In the southern regions, including Gulf of St. Lawrence, Scotian shelves, Gulf of Maine and MAB, the seasonal changes in sea level are more moderate in the range of about 5 cm between June and December. This regional difference reflects not only the larger magnitude of seasonal variability in wind stress in the northern coast, such as in the Labrador Sea, but also the pattern of seasonal changes between two broad regions—north and south of Laurentian Channel. In the southern region, the wind stress intensifies in fall/winter, just as in the northern region, but the intensified wind is oriented in a direction that is perpendicular to the coast (Figure 11). In contrast, the wind stress in the northern region not only becomes stronger in fall/winter but also remains in direction that is mostly parallel to the coast. Therefore, the impact of the seasonally intensified wind in the northern region is more effective in setting up cross-shelf coastal sea level tilt through Ekman dynamics. Furthermore, the local sea level setup has a far-reaching impact for the along-shelf flow downstream. The modeled (this study, Figure 9) and observed (Lentz 2008b) seasonal variation of shelf transport potentially reflects the changes of the along-shelf sea level tilt.

3.3. Influences of Open-Ocean Forcing

According to barotropic dynamics, the continental slope is an effective potential vorticity (PV) barrier that may insulate shelf circulation from open-ocean influences (e.g., Chapman, 1986; Wang, 1982). The open-ocean forcing becomes effective when the PV barrier is weakened and/or ageostrophic processes are strengthened at the shelf break (e.g., Brink, 1998, 2016). Both factors are sensitive to bathymetric features, background circulations and external forcings. To test the role of shelf-slope exchanges with realistic bathymetry, we designed and conducted an experiment using our two-layer model in which the atmospheric forcing (wind stress) is turned off and the coastal region (between coast and 1,500 m isobath) of the model is forced by an open-boundary condition along the 1,500 m isobath. All model variables along the open boundary are specified from that in the control run at each time step. As in the control run, the model is integrated for 100 years and the 100th year result is used for analyses. The open boundary condition along the 1,500 m isobath represents mainly boundary currents of open-ocean gyres. However, it is also affected by wind stress on shelves in the control run.

In the NWA region the most salient open ocean processes are wind-driven subtropical and subpolar gyres as shown in the annual-mean SSH field (Figure 4). On the NWA shelves north of Cape Hatteras, the circulation is more prone to influences from subpolar gyres than subtropical gyres because of information propagates in the downwave direction, that is, equatorward. Influences of Gulf Stream intrusion on shelves would affect regions that are southward of intrusion points. In our model, the Gulf Stream separates from the boundary around 37°N–38°N, its effects on shelves circulation is probably limited in the MAB region. We would like to note that this study focuses on interactions of mean flows and does not consider how mesoscale processes, such as the impingements of warm core rings, affect shelf circulations.

Figure 12 compares the annual-mean velocity between the coast and 1,000 m isobath between the control run (left panel) and the open-ocean forcing experiment (right panel). It is found that the cross-shelf intrusion from the deep ocean in the open-ocean forcing experiment (right panel) is most significant along the coasts of Labrador and Newfoundland and, therefore, we will focus our discussion in these regions. The annual-mean circulation from this experiment is an equatorward flow along the continental slope and on outer shelves, resembling that in the control run. There are several noticeable intrusions of the slope water into several deep channels between Nain Bank and Hamilton Bank. The intruded water flows cyclonically

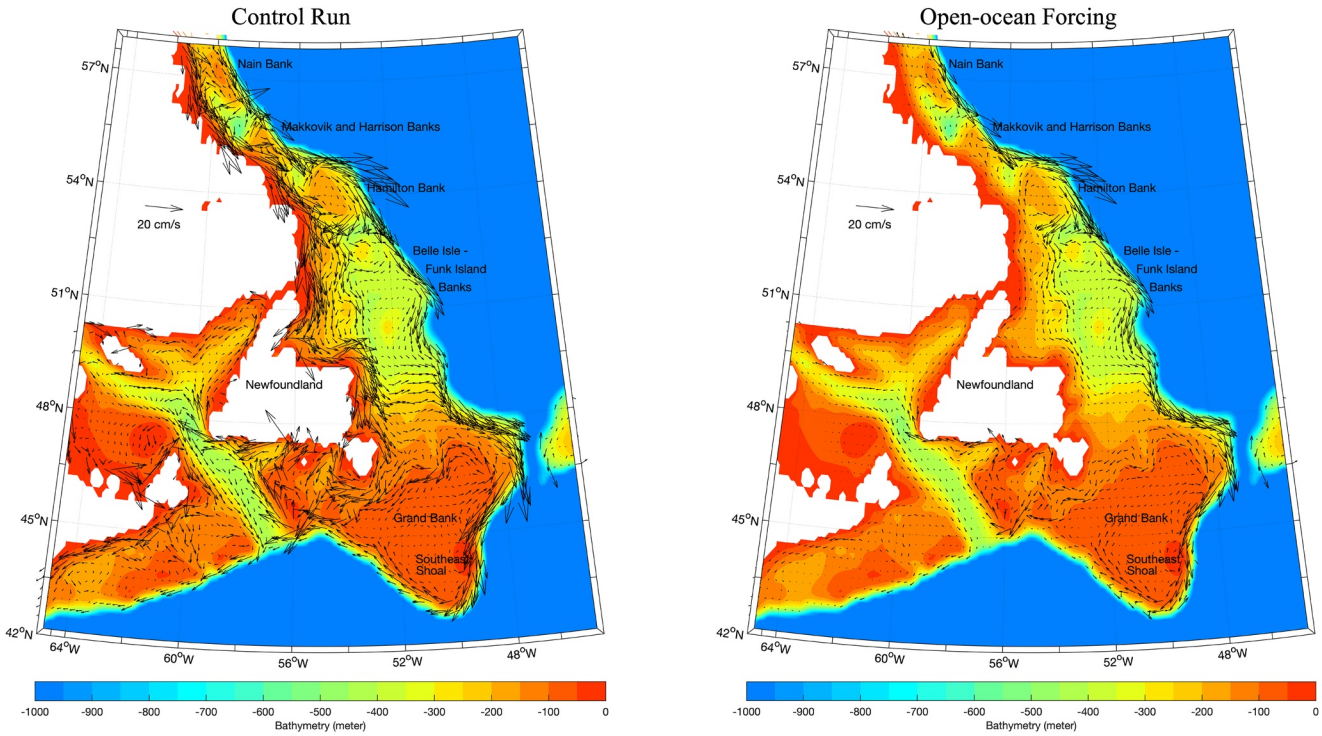

Figure 12. The annual-mean velocity between the coast and 1,000 m isobath from the control run (left panel) and the open-ocean forcing experiment in which the model is forced by the deep-ocean processes through an open boundary condition along 1,500 m isobath (right panel). The background color is the bathymetry (meters).

along the geostrophic contours, that is, isolines of f/h (Figure 13), and exit deep channels to re-join the slope current. Such intrusion did not induce significant flows across f/h isolines. There is a strong westward flow along the southern Hamilton Bank along f/h isolines toward the Newfoundland shelves. It turns southward along isobaths of 200–300 m toward the northern flank of the Grand Banks. The southward flow then bifurcates at about 48°N. One branch goes eastward along f/h isolines to the north of Grand Banks and then re-joins the slope current on the eastern side of Grand Banks. The other branch flows northward along 100–200 m isobaths to as far north as Makkovik and Harrison Banks.

The most significant cross-isobathic flows occur along the shelf break and continental slope around the Grand Banks. An onshore intrusion occurs just north of Southeast Shoal to form cyclonic flows along 100–150 m isobaths around Grand Bank. To the south of Southeast Shoal, the slope current moves upslope and flows anti-cyclonically at the depth of around 100 m. Observations are insufficient to characterize the cross-shelf intrusions along the Grand Banks's shelf break and the formation of the cyclonic shelf flows on Grand Banks. Our results appear to be consistent with those from data-assimilated models and realistic GCM simulations (e.g., Figure 13 from Han et al., 2008; Figure 8 from Wu et al., 2012; and Figure 4 from Wang et al., 2015). The cyclonic and anticyclonic flows merge off the southeast coast of Newfoundland and form a northwestward flow along the northern Laurentian Channel into the Gulf of St. Lawrence. An exit current flows southeastward along the southern Laurentian Channel and continues equatorward onto the Scotian shelf and into the Gulf of Maine. In summary, the wind-driven processes in the deep ocean, i.e., defined as 1,500 m and deeper in our study, exert a significant influence on shelf circulations especially in around the Grand Banks and Newfoundland shelves. The cross-shelf intrusion is particularly noticeable around the Hamilton and Grand Banks. The continental slope is steep and narrow along the eastern and southern Grand Banks, as evident in the f/h contours in Figure 13. A water parcel in a geostrophic flow moves along isoline of f/h to preserve its planetary PV. When the width of slope narrows frictional effects become important and ageostrophic velocity across f/h contours would intensify (e.g., Yang et al., 2013). In an extreme scenario, a slope current would be governed by frictional western boundary layer dynamics if the width of slope approaches either Stommel or Munk boundary layer scale. The Munk and Stommel WBL

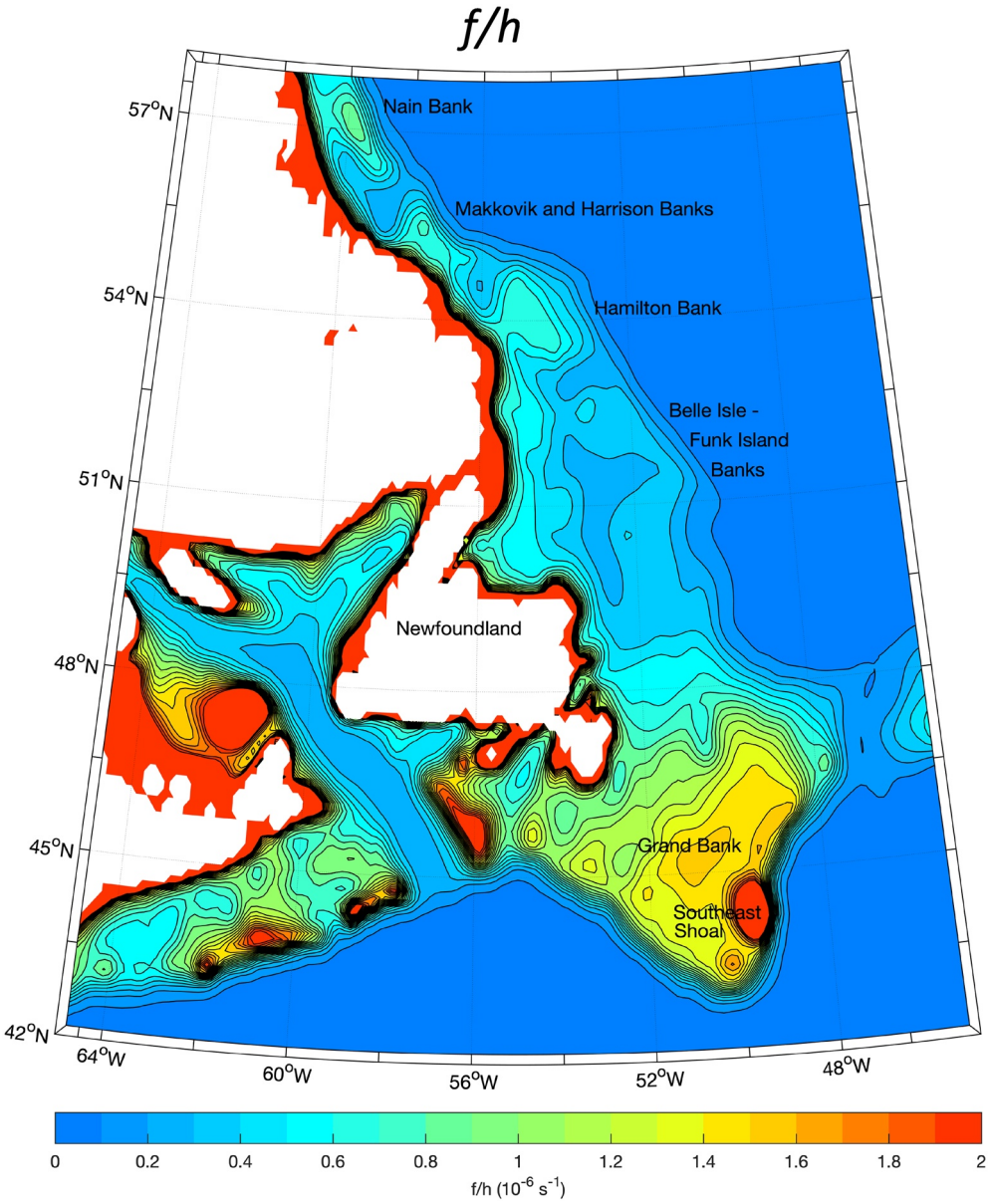

Figure 13. Contours of f/h, where h is the water depth and f is the planetary vorticity. The contour interval is 0.1×10^{-6} m^{-1}s^{-1}. The width of continental slope is narrow around the Grand Banks and so the cross-isobathic gradient of f/h is large there.

width at 45°N for the model parameters ($A = 500$ m^2 s^{-1}, $C_d = 1 \times 10^{-3}$, $|u| \sim 0.5$ ms^{-1} and $H \sim 1{,}000$ m) are about 30–50 km. At 50°W the water depth changes from 300 m on to 2,000 m over Grand Banks slope over a distance of about 40 km, about the same as the Munk or Stommel WBC width. It is postulated here that frictional processes have play an important role for promoting cross-isobath flows along the shelf break of Grand Banks.

3.4. Local Wind-Stress Forcing on the Shelves

The along-shelf sea-level gradient is important for maintaining the along-shelf mean flow on the NWA shelf. The origin of the gradient, however, needs to be better understood, although it is well recognized that freshwater flux is a main contributor (Chapman & Beardsley, 1989). The freshwater flux contributes to sea

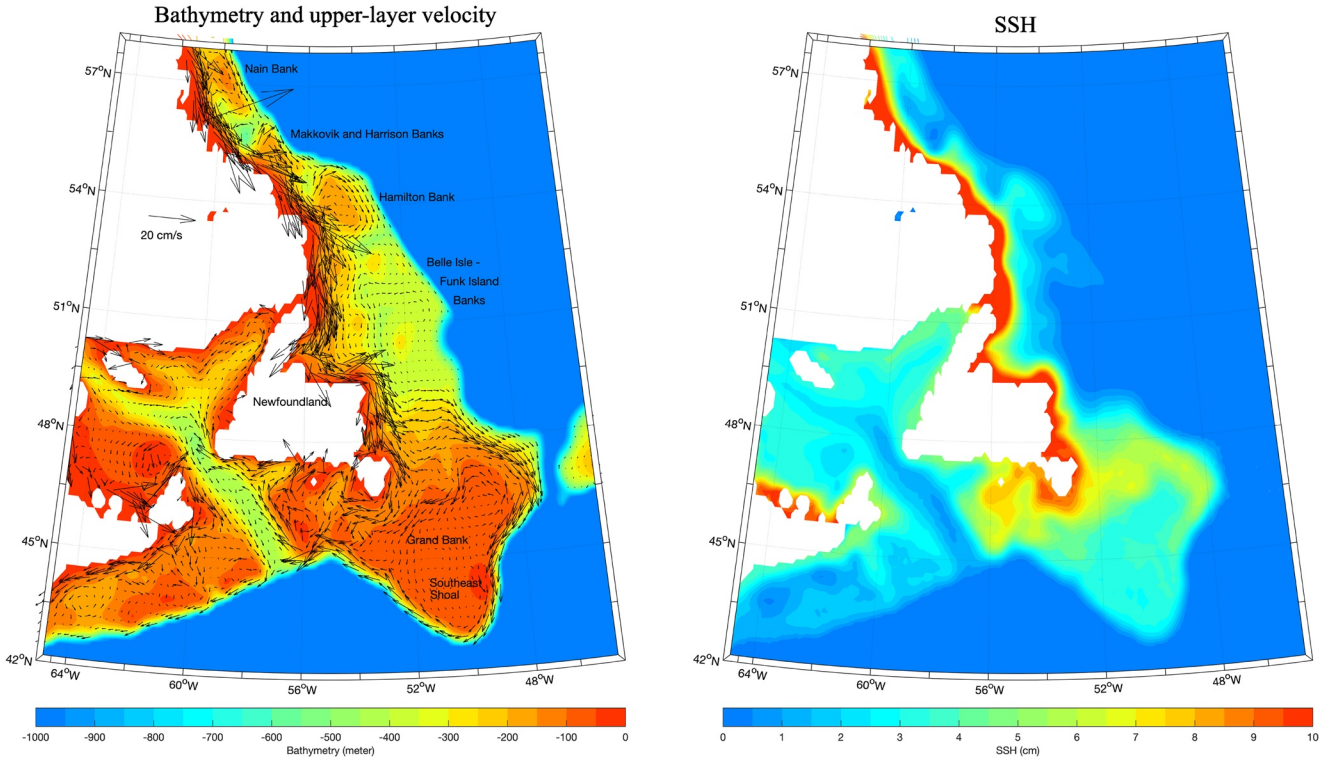

Figure 14. (left) the annual-mean velocity between the coast and 1,000 m isobath from an experiment in which the model is forced only by wind stress in areas shallower than 1,500 m. The deep-ocean processes, such as the subtropical and subpolar gyres, are excluded; and (right) the sea level (unit cm).

level change because it is a source of volume flux (although river runoff is typically small when compared with coastal current transport) and because it decreases the water density and thus elevates the steric height (e.g., Lazier & Wright, 1993 for their estimate of steric effect on the Labrador shelf). The sea level, however, can also be changed due to the convergence and divergence of the Ekman transport. A strong equatorward along-shore wind stress would lead to onshore Ekman transport, result in elevated sea level and contribute to the along-shelf sea-level gradient. Such favorable wind conditions are evident along the coast of Labrador and Baffin Island and along Hudson Strait (Figure 2).

To test the effectiveness of such a wind forcing, we have conducted another experiment by applying the wind stress forcing only between the coast and 1,500 m isobath. It is noted here that this specification of forcing may result in an artificial wind-stress curl and thus flow along 1,500 m isobath. We have conducted several additional experiments using different isobaths, that is, 2,000 and 2,500 m, as the offshore boundary for specifying the wind stress forcing. The velocity field in shallow water between the coast and 1,000 m isobath is essentially the same among all experiments. The impact of this artificial curl on shelf flow appears to be small in the model. Figure 14 shows the annual-mean fields of velocity (left) and sea level (right) in the region from Scotian to Labrador shelves between 42°N and 58°N. The sea level is high along the coast of Labrador and Newfoundland, which is resulted from a convergence of the onshore Ekman transport driven by the equatorward along-shore wind stress. The sea level decreases equatorward along the coast because the wind stress forcing weakens southward. The sea-level difference between Labrador and Nova Scotia coasts is about 10 cm with an along-shore gradient about 5×10^{-8}. The main momentum balance in the along-isobath direction l is among the sea-level gradient, wind stress and bottom drag, that is,

$$-g\frac{\partial \eta}{\partial l} + C_d \frac{|v|v}{h} + \frac{\tau^l}{\rho h} = 0. \tag{4}$$

The annual-mean wind stress on shelves is on the order of 0.1 N/m^2. At the 100 m isobath, the magnitudes of the first two terms in (4) are about 5×10^{-7} and 1×10^{-6} respectively. Equation 4 would require a bottom drag associated with a velocity of about 0.38 m/s at 100 m isobath in order for the bottom drag to balance

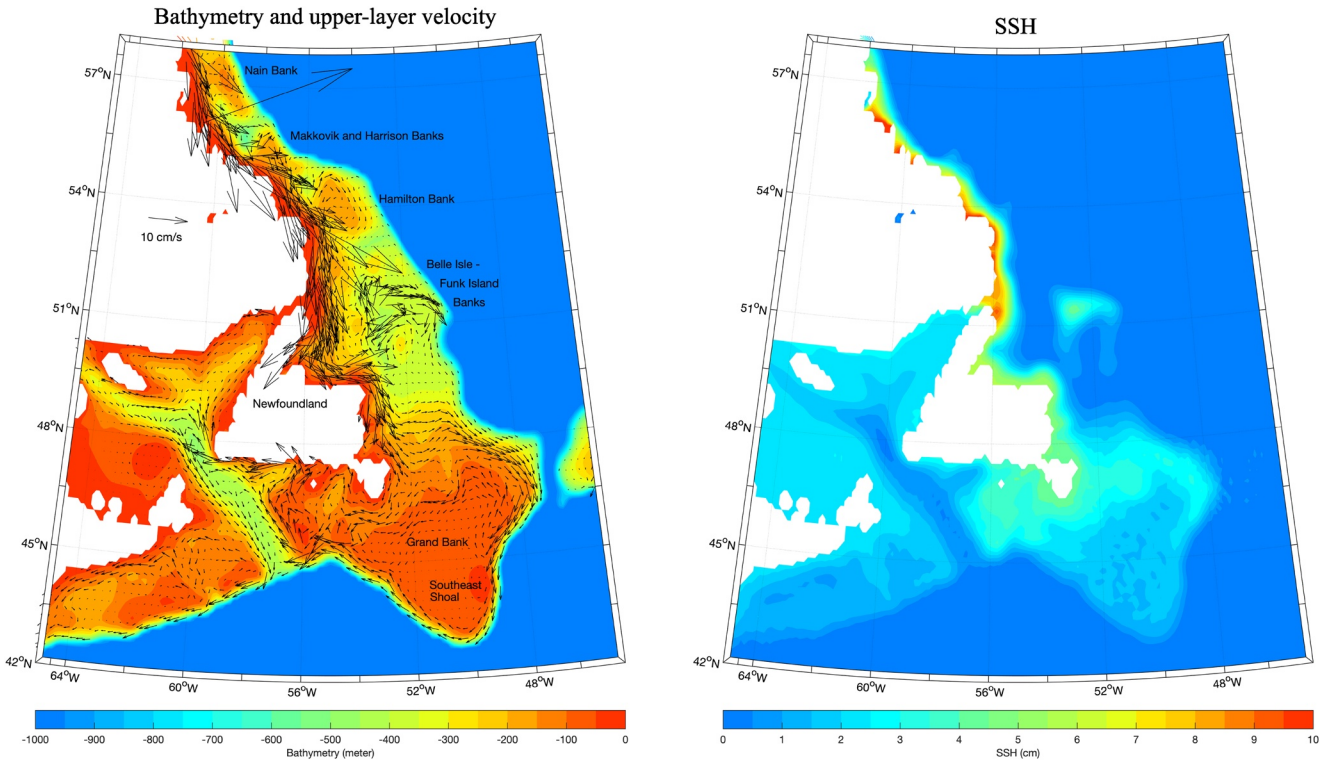

Figure 15. (left) annual mean velocity and (right) sea level height (unit: cm) from an experiment in which wind-stress forcing is applied only in the Labrador shelves between the coast and 1,500 m isobath from 50°N to 60°N (the vector sizes are different from that in Figure 14). The experiment shows the effectiveness of remote forcing on downwind regions from Newfoundland shelves to MAB.

the local wind stress and sea-level gradient. The model velocity field, shown in Figure 14, is consistent with this estimate.

Figure 14 shows the overall impacts of wind stress forcing on the shelf circulation on the Labrador and Newfoundland shelves. We have conducted several additional experiments to identify where on the shelves the forcing is more effective to regional circulations. It is found that the forcing on Labrador shelves have the most significant impacts on shelf circulation along the US and Canada coast from Labrador coast to Cape Hatteras. Figure 15 shows the annual velocity and sea level in an experiment in which is forcing is applied only between the coast and 1,500 m isobath in a small region of Labrador shelves between 50°N and 60°N. This high-latitude forcing induces sea-level gradient and along-shelf flows all the way to MAB (note that the vector scale in Figure 15 is different from that in Figure 14). In this experiment, the mean along-shelf transports in MAB, Gulf of Maine, Laurentian Channel, Scotian and Newfoundland shelves are about 40%–60% of the transport in the experiment shown in Figure 14 even though there is no local forcing in these regions. It shows that the wind stress forcing on Labrador shelves is as important as the local wind stress for the mean shelf flow north of the MAB. Additional experiments (not shown) indicate that wind stress on Newfoundland and Scotian shelves also remotely forces flows in the downwind regions. Exchange flow through Hudson Strait is mainly forced by the along shore wind in the southern Hudson Bay and along Baffin Island's coast. Local wind stress forcing is less important in the MAB, Gulf of Maine and Scotian shelves. Local wind forcing along Laurentian Channel and in Gulf of St. Lawrence is important in fall and winter season and weak in the summer when surface wind stress weakens.

The results from our simple model highlights the importance of wind-driven process in driving the along-shelf flow from the Labrador shelf to the MAB. The strong along-shelf wind on the Labrador shelf sets up sea level gradient in both the cross-shelf and along-shelf direction, which both drives an along-shelf flow. While the cross-shelf pressure gradient may be local, the along-shelf sea level gradient can be felt further downstream.

4. Summary

In this study, we use a two-layer model to examine wind-driven flows on the NWA shelves. The results indicate that the wind forcing alone is able to drive an equatorward along-shelf flow from Greenland's southern coast to north of Cape Hatteras. The regional details of the modeled shelf circulation are remarkably similar to what is characterized and quantified from observations. The along-shelf sea-level gradient in the MAB and Scotian shelf is almost identical to 3.7×10^{-8}, which is estimated from observations (Lentz, 2008a). The along-shelf flow is strengthened in fall/winter and weakened in spring/summer due to the seasonal variability of along-shelf wind especially in areas off Newfoundland and Labrador coast. The wind stress affects the along-isobath flows through two processes. First, it affects the along-shelf momentum balance that, according Equation 4, is maintained by the along-shore sea-level gradient, along-shelf wind stress and the bottom drag. If the sea-level gradient is set up by non-local processes at its origins in upstream regions, a change in wind stress locally would have to be balanced mainly by changes in bottom drag so that the momentum balance is maintained. A seasonally strengthened along-shelf wind in the equatorward direction in fall/winter, for instance, would require an enhanced bottom friction in the opposite direction. This would result in a stronger equatorward flow. Second, the along-shore wind forces a convergence or divergence of the surface Ekman transport. An equatorward along-shore wind forces an onshore Ekman transport and result in elevated sea level. The onshore Ekman transport is particularly strong along the coast of Labrador and Newfoundland, and is a primary cause for the mean along-shore sea-level gradient that extends from Hudson Strait to MAB in our model.

We conduct additional numerical simulations to examine the relative contributions from direct wind forcing on shelves and from influences from open-ocean gyres through their WBCs. The local forcing on shelves is more dominant for flows in shallower waters near the coast while open-ocean forcing is effective for flows along the outer shelf. Cross-isobath flows are induced by ageostrophic processes. It is found in the model simulations that the intrusion from deep ocean to shelves are particularly strong around the Grand Banks. The width of the continental slope there is similar to the width of a frictional WBC. It is postulated that friction may play an important role in promoting cross-isobath flows there.

This study shows that the wind stress alone is able to drive a shelf flow that compares well with observations both qualitatively and quantitatively. This indicates that the wind stress is likely as important as the buoyancy forcing for the mean NWA shelf circulations. One objective of this study is to motivate more studies using models that have both wind and buoyancy forcings. The bottom friction is a leading term for the along-shelf momentum balance. With buoyancy forcing there will be a thermal wind shear due to the cross-shelf density gradient. This shear will definitely affect the bottom geostrophic velocity and thus the bottom friction. It remains to be investigated how the results from this model might be altered if buoyancy forcing is additionally considered. We would also like to point out that our model is forced by the long-term climatological wind stress that most likely already filters out sporadic events like storms. The effects of synoptic wind-stress forcing of the mean flow on shelves remain to be studied. In addition, our model does not include sea-ice covers. High-latitude shelves, such as Labrador and Newfoundland shelves, are covered by sea ice in winter. The ice coverage may alter the momentum fluxes and thus affect the wind-driven shelf flows in winter. A further study is needed to assess the sea-ice effects.

Acknowledgement
Both Yang and Chen are also supported by NOAA Climate Program Office's Climate Variability and Prediction Program under grant NA20OAR4310398. JY is supported by Woods Hole Oceanographic Institution (WHOI) W. V. A. Clark Chair for Excellence in Oceanography and NSF Ocean Science Division under grant OCE1634886. Chen is supported by WHOI Independent Research and Development award. During the course of this study the authors have benefited from discussions with Drs. Steve Lentz and Ken Brink. The authors would also like to thank three reviewers for their constructive comments that have helped improving the manuscript.

Data Availability Statement

The ERA Interim wind-stress climatology is publicly accessible at https://www.ecmwf.int/en/forecasts/datasets, and the ETOPO 5 bathymetry data used in the model is from https://www.ngdc.noaa.gov/mgg/global/relief/ETOPO5. The model outputs and plotting programs are accessible at: https://doi.org/10.5281/zenodo.4456293.

References

Anderson, D. T. L., & Gill, A. E. (1975). Spin-up of a stratified ocean, with applications to upwelling. *Deep Sea Research*, *22*, 583–596.
Beardsley, R. C., & Winant, C. D. (1979). On the mean circulation in the Mid-Atlantic bight. *Journal of Physical Oceanography*, *9*, 612–619. https://doi.org/10.1175/1520-0485(1979)009<0612:otmcit>2.0.co;2
Brink, K. H. (1998). Deep-sea forcing and exchange processes. In K. H. Brink, & A. R. Robinson (Eds.), *The Sea*. John Wiley.

Brink, K. H. (2016). Cross-Shelf Exchange. *Annual review of marine science*, *8*, 59–78. https://doi.org/10.1146/annurev-marine-010814-015717
Chapman, D. C. (1986). A simple model of the formation and maintenance of the shelf/slope front in the Middle Atlantic Bight. *Journal of Physical Oceanography*, *16*, 1273–1279. https://doi.org/10.1175/1520-0485(1986)016<1273:asmotf>2.0.co;2
Chapman, D. C., & Beardsley, R. C. (1989). On the origin of shelf water in the Middle Atlantic Bight. *Journal of Physical Oceanography*, *19*, 384–391. https://doi.org/10.1175/1520-0485(1989)019<0384:otoosw>2.0.co;2
Chassignet, E. P., & Marshall, D. P. (2013). Gulf stream separation in numerical ocean models. In M. W. Hecht, & H. Hasumi (Eds.), *Ocean modeling in an eddying regime, Geophysical Monograph Series*. Washington, DC: American Geophysical Union. https://doi.org/10.1029/177GM05
Csanady, G. T. (1976). Mean circulation in shallow seas. *Journal of Geophysical Research*, *81*, 5389–5399. https://doi.org/10.1029/jc081i030p05389
Csanady, G. T. (1978). The Arrested Topographic Wave. *Journal of Physical Oceanography*, *8*, 47–62.
Csanady, G. T. (1982). *Circulation in the coastal ocean*. Springer.
Csanady, G. T. (1985). "Pycnobathic" currents over the upper continental slope. *Journal of Physical Oceanography*, *15*, 306–315. https://doi.org/10.1175/1520-0485(1985)015<0306:cotucs>2.0.co;2
Dickson, R., Meincke, J., & Rhines, P. (2008). *Arctic-Subarctic ocean fluxes, pp736*. Springer.
Han, G., Lu, Z., Wang, Z., Helbig, J., Chen, N., & de Young, B. (2008). Seasonal variability of the Labrador Current and shelf circulation off Newfoundland. *Journal of Geophysical Research*, *113*. https://doi.org/10.1029/2007jc004376
Hannah, C. G., Shore, J. A., Loder, J. W., & Naimie, C. E. (2001). Seasonal circulation on the western and central Scotian Shelf. *Journal of Physical Oceanography*, *31*, 591–615. https://doi.org/10.1175/1520-0485(2001)031<0591:scotwa>2.0.co;2
Lazier, J. R. N., & Wright, D. G. (1993). Annual velocity variations in the Labrador Current. *Journal of Physical Oceanography*, *23*, 659–678. https://doi.org/10.1175/1520-0485(1993)023<0659:avvitl>2.0.co;2
Lentz, S. J. (2008a). Observations and a model of the mean circulation over the middle Atlantic bight continental shelf. *Journal of Physical Oceanography*, *38*, 1203–1221. https://doi.org/10.1175/2007jpo3768.1
Lentz, S. J. (2008b). Seasonal Variations in the Circulation over the Middle Atlantic Bight Continental Shelf. *Journal of Physical Oceanography*, *38*, 1486–1500.
Ma, C., Wu, D., Lin, X., Yang, J., & Ju, X. (2010). An open-ocean forcing in the East China and Yellow seas. *Journal of Geophysical Research: Oceans*, *115*. https://doi.org/10.1029/2010jc006179
Pringle, J. M. (2018). Remote forcing of shelf flows by density gradients and the origin of the annual mean flow on the Mid-Atlantic Bight. *Journal of Geophysical Research: Oceans*, *123*, 4464–4482. https://doi.org/10.1029/2017jc013721
Saucier, F. J., Senneville, S., Prinsenberg, S., Roy, F., Smith, G., Gachon, P., et al. (2004). Modelling the sea ice-ocean seasonal cycle in Hudson Bay, Foxe Basin and Hudson Strait, Canada. *Climate Dynamics*, *23*, 303–326. https://doi.org/10.1007/s00382-004-0445-6
Scott, J. T., & Csanady, G. T. (1976). Nearshore currents off long Island. *Journal of Geophysical Research*, *81*, 5401–5409. https://doi.org/10.1029/jc081i030p05401
Stommel, H., & Leetmaa, A. (1972). Circulation on the continental shelf. *Proceedings of the National Academy of Sciences*, *69*, 3380–3384. https://doi.org/10.1073/pnas.69.11.3380
Townsend, D. W., Pettigrew, N. R., Thomas, M. A., Neary, M. G., McGillicuddy, D. J., Jr, & O'Donnell, J. (2015). Water masses and nutrient sources to the Gulf of Maine. *Journal of Marine Research*, *73*, 93–122. https://doi.org/10.1357/002224015815848811
Vennell, R., & Malanotte-Rizzoli, P. (1987). Coastal flows driven by alongshore density gradients. *Journal of Physical Oceanography*, *17*, 821–827. https://doi.org/10.1175/1520-0485(1987)017<0821:cfdbad>2.0.co;2
Wang, D.-P. (1982). Effects of continental slope on the mean shelf circulation. *Journal of Physical Oceanography*, *12*, 1524–1526. https://doi.org/10.1175/1520-0485(1982)012<1524:eocsot>2.0.co;2
Wang, Z., Yashayaev, I., & Greenan, B. (2015). Seasonality of the inshore Labrador current over the Newfoundland shelf. *Continental Shelf Research*, *100*, 1–10. https://doi.org/10.1016/j.csr.2015.03.010
Wu, Y., Tang, C., & Hannah, C. (2012). The circulation of eastern Canadian seas. *Progress in Oceanography*, *106*, 28–48. https://doi.org/10.1016/j.pocean.2012.06.005
Xu, F.-H., & Oey, L.-Y. (2011). The origin of along-shelf pressure gradient in the Middle Atlantic Bight. *Journal of Physical Oceanography*, *41*, 1720–1740. https://doi.org/10.1175/2011jpo4589.1
Yang, J. (2015). Local and remote wind stress forcing of the seasonal variability of the Atlantic meridional overturning circulation (AMOC) transport at 26.5°N. *Journal of Geophysical Research: Oceans*, *120*, 2488–2503. https://doi.org/10.1002/2014jc010317
Yang, J., Lin, X., & Wu, D. (2013). Wind-driven exchanges between two basins: Some topographic and latitudinal effects. *Journal of Geophysical Research: Oceans*, *118*, 4585–4599. https://doi.org/10.1002/jgrc.20333
Yang, J., & Pratt, L. J. (2013). On the effective capacity of the dense-water reservoir for the Nordic Seas overflow: Some effects of topography and wind stress. *Journal of Physical Oceanography*, *43*, 418–431. https://doi.org/10.1175/jpo-d-12-087.1
Yang, J., & Pratt, L. J. (2014). Some dynamical constraints on upstream pathways of the Denmark strait overflow. *Journal of Physical Oceanography*, *44*, 3033–3053. https://doi.org/10.1175/jpo-d-13-0227.1